

# High-Frequency CubeSat Platform Scattering Using Higher-Order Method of Moments

Jakob Rosenkrantz de Lasson, Oscar Borries, Cecilia Cappellin, and Tonny Rubæk  
TICRA, Landemærket 29, DK-1119 Copenhagen K, Denmark, {jrdl,ob,cc,tr}@ticra.com

**Abstract**—We present a 10 cm offset reflector antenna mounted inside a 6U CubeSat platform and analyze the bare reflector and three reflector + CubeSat platform configurations in W band (86 GHz), where the CubeSat platform is electrically large. Using higher-order MoM/MLFMM techniques, we obtain accurate antenna patterns and quantify the significant impact that any of the CubeSat platforms in this case have on the antenna pattern. In addition, our study demonstrates that details of the CubeSat platform impact the patterns to a lot smaller extent.

## I. INTRODUCTION

Conventional satellites and spacecrafts are expensive and time-consuming to develop and launch into space, and in recent years smaller satellites, commonly referred to as *Small-Sats*, have emerged as a cheaper and faster-to-develop alternative. Such small satellites may find both commercial and scientific applications, and as a prominent example mega-constellations, consisting of hundreds or thousands of Small-Sats, may become a new paradigm in telecommunication.

A particular class of SmallSat is *CubeSats* that are made of  $10 \times 10 \times 10 \text{ cm}^3$  units, the CubeSat unit (1U). As an example, a collection of  $3 \times 2 \times 1$  units is called a 6U CubeSat. While CubeSats started out as cheap and accessible test beds at universities, they now also find widespread commercial use [1]. A recent example of the use of CubeSats was the 6U Mars Cube One (MarCO) [2], which was part of NASA's InSight mission to Mars.

Many CubeSat missions have used antennas in UHF, S and Ka bands [1], where the comparatively small CubeSat platform remains modest in electrical size. In higher frequency bands, such as W band that may become important in future broadband and high-capacity satellite communication [3], treating accurately the electrically large CubeSat platform as part of RF antenna design and validation is not straightforward.

In this work, we present an accurate and efficient full-wave solution of the CubeSat platform scattering problem for a reflector antenna in W band. We compare the bare antenna pattern to that in the presence of a 6U CubeSat and illustrate the impact from platform scattering for three CubeSat platform configurations. For RF analyses, we use the MoM add-on to the GRASP software [4], which discretizes the geometry using higher-order quadrilateral patches and surface currents using higher-order basis functions. This combination makes it particularly suited for electrically large structures, and its feasibility for conventional telecommunication satellites has already been demonstrated at lower frequencies [5].

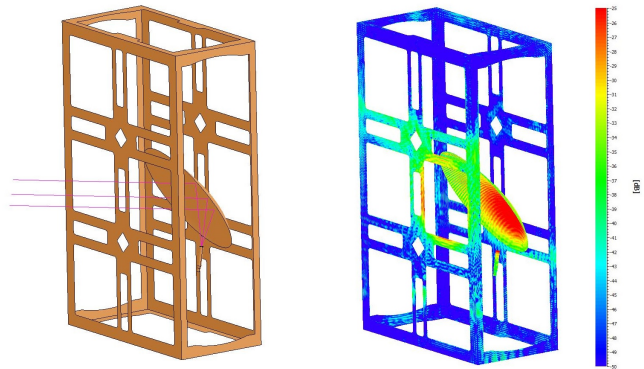


Fig. 1. Single-offset reflector antenna inside 6U CubeSat chassis. *Left:* Reflector and CubeSat chassis. Selected rays from feed are shown. *Right:* Simulated MoM currents on entire structure at 86 GHz.

## II. REFLECTOR AND CUBE SAT PLATFORM

We consider an offset reflector intended for CubeSat applications, with projected aperture diameter of  $D = 10 \text{ cm}$ , normalized focal length of  $f/D = 0.25$  and no clearance ( $d' = 0$ ). The relatively small focal length ensures a compact antenna fitting inside the 6U CubeSat chassis, see Fig. 1. We consider a W-band frequency of 86 GHz, at which the CubeSat chassis has outer dimensions of  $(29, 57, 86)\lambda$ . As feed, we use a circularly polarized (LHC) tapered waveguide with aperture diameter of 3.2 mm. The reflector, feed and position inside the CubeSat chassis are inspired by [6].

## III. ANTENNA PATTERNS AND PLATFORM SCATTERING

Computed currents on the reflector and CubeSat platform are displayed in the right part of Fig. 1, a computation that ran on a laptop and required 6 GB of RAM. Figure 2 displays RHC (black) and LHC (magenta) directivity patterns, with dashed (solid) curves being for the bare reflector (full structure). The left [right] panel are patterns in the  $\phi = 0^\circ$  [ $\phi = 90^\circ$ ] plane.

Both patterns exhibit the characteristic beam squint in the  $\phi = 90^\circ$  plane, and the bare reflector has a peak directivity of 36.54 dBi (37.42 dBi) in the  $\phi = 0^\circ$  ( $\phi = 90^\circ$ ) plane. The full structure has a peak directivity that is 1.3 to 1.4 dB lower (see Table I), and its RHC sidelobes are substantially higher than for the bare reflector. The LHC patterns are not changed significantly due to the introduction of the CubeSat platform. However, the changes of the RHC pattern represent significant degradations in typical scenarios, and with the MoM/MLFMM solution presented here it is possible to obtain accurate infor-

mation about the impact from the CubeSat platform, also at the high frequency considered here.

TABLE I  
PEAK DIRECTIVITY FOR BARE REFLECTOR AND THREE REFLECTOR + CUBE-SAT PLATFORM CONFIGURATIONS.

[dBi]	Bare Reflector	Reflector + Platform		
		Open	Partially Closed	Closed
$\phi = 0^\circ$	36.54	35.25	35.24	35.01
$\phi = 90^\circ$	37.42	36.01	36.02	35.69

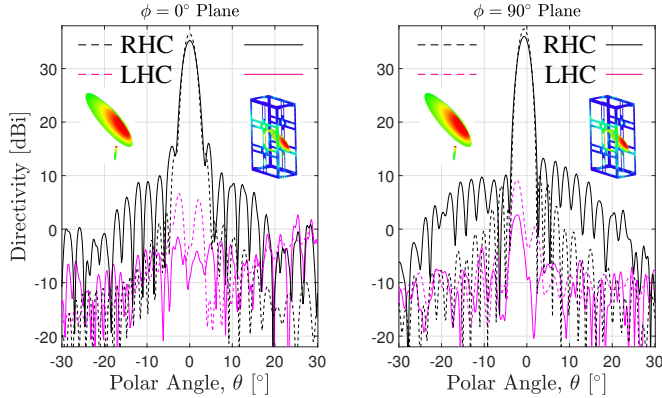


Fig. 2. Directivity patterns. Black (magenta) curves are RHC (LHC), dashed [solid] curves are for the bare reflector (reflector + CubeSat platform).

In a practical scenario, the CubeSat platform chassis will not be open as shown in Fig. 1, but will be partially or fully closed to shield and protect electronics and other components inside. Therefore, we consider, in addition to the open chassis, partially and fully closed configurations, the latter of these only containing the hole right in front of the reflector. The three CubeSat chassis configurations are displayed in the top part of Fig. 3. The bottom part of the figure displays RHC directivity patterns for the three configurations, with the left (right) panel being in the  $\phi = 0^\circ$  ( $\phi = 90^\circ$ ) plane.

The difference between these three sets of patterns is substantially smaller than that observed in Fig. 2, implying that introducing *any* CubeSat platform affects the antenna patterns much more than the details of this platform. This being said, we do note slightly higher sidelobes and a decrease of the peak directivity of about 0.3 dB for the closed CubeSat platform chassis as compared to the open and partially closed ones (see Table I). A recent study showed that computation of antenna patterns with ray tracing in a partially closed and electrically large structure is less accurate than the MoM/MLFMM approach adopted here [7].

#### IV. CONCLUSION

We have presented and analyzed an offset reflector antenna inside three 6U CubeSat platform configurations. All analyses have been carried out in W band (86 GHz), where the CubeSat platform is electrically large, and where accurate analysis of platform scattering therefore is not straightforward. Using the MoM add-on to the GRASP software, which discretizes the geometry using higher-order quadrilateral patches and surface

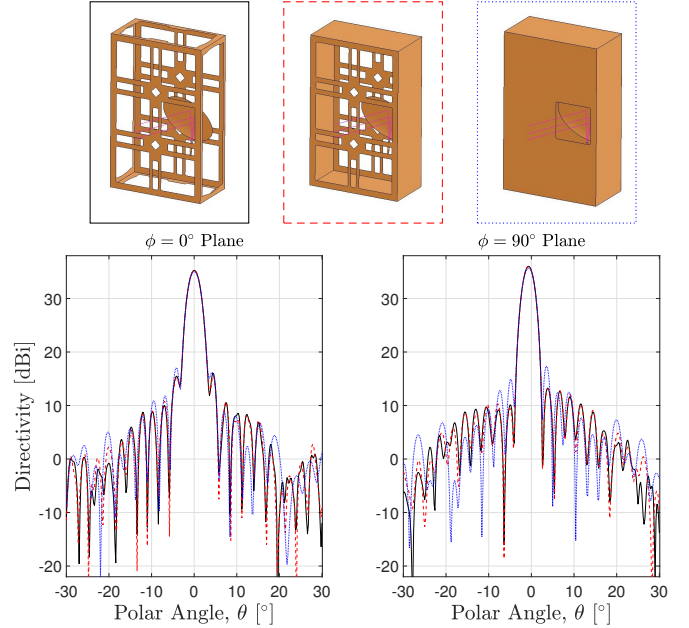


Fig. 3. *Top*: Open (left, solid black), partially closed (center, dashed red) and closed (right, dotted blue) CubeSat platform chassis. *Bottom*: Co-polar (RHC) directivity patterns in principal planes of reflector + each of the three CubeSat platform configurations.

currents using higher-order basis functions, we have analyzed the bare reflector and three reflector + CubeSat platform configurations and presented the associated antenna patterns. We found, in the example studied here, a strong impact on the pattern from introducing any of the CubeSat platform configurations, while using an open, a partially closed or a closed CubeSat chassis only produced minor changes to the patterns. Our results illustrate that CubeSat platform scattering can be accurately accounted for by using MoM/MLFMM, even at higher frequencies that will become technologically and commercially relevant in the future.

#### REFERENCES

- [1] Y. Rahmat-Samii, V. Manohar, and J. M. Kovitz, "Think small, dream big: A review of recent antenna developments for CubeSats," *IEEE Antennas Propag. Mag.*, vol. PP, no. 99, pp. 1–1, 2017.
- [2] R. E. Hodges, N. Chahat, D. J. Hoppe, and J. D. Vacchione, "A deployable high-gain antenna bound for Mars: Developing a new folded-panel reflectarray for the first CubeSat mission to Mars," *IEEE Antennas Propag. Mag.*, vol. 59, no. 2, pp. 39–49, April 2017.
- [3] M. Lucente, T. Rossi, A. Jebiril, M. Ruggieri, S. Pulitano, A. Iera, A. Molinaro, C. Sacchi, and L. Zuliani, "Experimental missions in W-Band: A small LEO satellite approach," *IEEE Systems Journal*, vol. 2, no. 1, pp. 90–103, March 2008.
- [4] GRASP Software, TICRA, Copenhagen, Denmark, www.ticra.com.
- [5] E. Jørgensen, O. Borries, P. Meincke, M. Zhou, and N. Vesterdal, "New fast and robust modelling algorithms for electrically large antennas and platforms," in *2015 9th European Conference on Antennas and Propagation (EuCAP)*, April 2015.
- [6] G. Mishra, A. T. Castro, S. K. Sharma, and J.-C. S. Chieh, "W-band feed horn with polarizer structure for an offset reflector antenna for CubeSat applications," in *Antennas and Propagation Society International Symposium*, 2017.
- [7] J. R. de Lasson, P. H. Nielsen, C. Cappellin, D. M. Alvarez, M. Bergada, R. Gonzalez, and P. de Maagt, "Full-wave and multi-GTD analysis of the Ice Cloud Imager for MetOp-SG," in *2017 11th European Conference on Antennas and Propagation (EuCAP)*, March 2017.